Hydraulic Permeability of Open-Cell Hydrophilic Polyurethane Foams

MICHAEL V. SEFTON and HARRIS M. LUSHER,* *Department of Chemical Engineering and Applied Chemistry, University of Toronto, Toronto, Ontario, M5S 1A4, Canada*

Synopsis

The hydraulic permeabilities of open-cell hydrophilic polyurethane (Hypol) foams have been measured at steady state over a pressure gradient range of 10^2–10^4 dyn/cm^3. These permeabilities were sensitive to the relative amounts of prepolymer, water, and surfactant, and to the mode of preparation. Furthermore, the noted sample-to-sample variations suggested that mixing effects were also significant. Inertial losses, viscous losses, and energy losses associated with the pushing aside of loose foam struts were apparent at high, low, and very low gradients, respectively. Over the gradient range investigated, compression of the foam was considered to be a minor factor in accounting for the decreased permeability at higher gradients. The viscous loss term or Darcian permeability was correlated with cell size using the Carman–Kozeny equation indicating that the major determinant of hydraulic permeability was pore size rather than porosity. The fiber drag model of flow through porous media was also used to account for the permeability in terms of strut diameter rather than cell size.

INTRODUCTION

Although the hydraulic permeability of certain open-cell materials used as membrane filters has been subject to detailed study,[1–4] there has been only limited investigation of the permeability of open-cell foams.[5,6] However, the diffusive permeability of blowing agents or water vapor in closed-cell foams[7–11] and benzene in open-cell foams,[12] has been studied.

The development of a controlled-release micropump for insulin delivery at variable rates[13,14] initiated this study of the hydraulic permeability of hydrophilic polyurethane foams (Hypol). A short rod of Hypol foam is used in this micropump to control the basal delivery of insulin to that which is required by the diabetic between meals. Rapid compression of the foam by the core of a solenoid augments the delivery to provide the insulin that is needed during or immediately after meals. This investigation was a prelude to a study of the effects of repeated compression on hydraulic permeability.

Hypol foams are based on the mixing of a polyisocyanate end-capped polyoxyethylene polyol with a molar excess of water.[15] A blowing agent is mixed with the end-capped polyol to yield the commercial prepolymer. The prepolymer used here, FHP3000 has an equivalent weight per isocyanate group of 400–450 and 2.2–2.5 mequiv/g of isocyanate. Unlike hydrophobic foaming systems, an excess of water is preferable for the best foams. For example, the recommended formulation[16] for a "nonwicking foam" involves the mixing of 100 parts by weight of prepolymer with 70 parts of water and one part of surfactant (L520); this

* Present address: Food Specialties Limited, Ajax, Ontario, Canada.

Journal of Applied Polymer Science, Vol. 25, 2167–2178 (1980)

0021-8995/80/0025-2167$01.20

corresponds to approximately 16.5 mol of water/mol of isocyanate. The cell size of the resulting foam (100/70/1) is approximately 0.2–0.5 mm. The cell size of other foams made with different amounts of the same reactants are significantly different as evidenced by the results presented here.

FLOW THROUGH POROUS MEDIA

Energy loss owing to viscous dissipation during flow through an incompressible porous material is accounted for in Darcy's law,

$$v = \frac{K}{\mu}\frac{\Delta P}{L_o} \tag{1}$$

where v = superficial velocity through the porous material, ΔP = pressure drop across the material, L_o = original length of material, μ = fluid viscosity, and K = Darcian permeability.

The Darcian permeability, K, can in turn be related to the structure of the foam through some model of foam structure. The most widely used is the Carman–Kozeny equation[17]:

$$K = \frac{\epsilon^3}{2\tau S^2(1-\epsilon)^2} = \frac{\epsilon^3}{A_c(1-\epsilon)^2} \tag{2}$$

where ϵ = porosity or void fraction, τ = tortuosity, a shape factor (here assumed $\tau = 1$), S = specific surface area of the matrix, and A_c = a constant for a given foam sample.

As derived, the Carman–Kozeny equation assumes that the foam can be described as a random packing of discrete particles characterized by a hydraulic pore radius expressed in terms of ϵ and S_o.

Alternatively, the foam can be visualized as a mat of randomly distributed fibers. The viscous drag on a fluid exerted by such a fibrous network is described by[18]:

$$K = \frac{3\epsilon\delta^2(4 - \ln \mathrm{Re}/\delta)}{16(1-\epsilon)(2 - \ln \mathrm{Re}/\delta)} = \frac{\epsilon}{A_f(1-\epsilon)} \tag{3}$$

where δ = characteristic fiber diameter, Re = Reynold's number = $\delta v\rho/\mu$, ρ = fluid density, and A_f = a constant for each foam sample.

According to this expression, permeability is much less dependent on porosity than suggested by eq. (3) [$K \propto \epsilon/(1-\epsilon)$ instead of $K \propto \epsilon^3/(1-\epsilon)^2$]. For eq. (3), A_f is slightly dependent on velocity.

In addition, the foams are compressible so that foam length decreases with increasing pressure and, more importantly, porosity decreases. Since the foams are restrained laterally during flow measurement, only uniaxial compression needs be considered so that

$$L = L_o(1 - \Delta P/E) \tag{4}$$

where L = foam length at pressure ΔP, L_o = foam length at zero pressure (original length), and E = compression modulus of the foam.

Since the volume of the swollen matrix is unchanged, it can be shown that

$$\epsilon = \frac{\epsilon_o - \Delta P/E}{1 - \Delta P/E} \tag{5}$$

where ϵ = porosity at pressure drop ΔP and ϵ_0 = porosity at zero pressure drop.

Although it was experimentally determined that the effect of compression on K was negligible, eqs. (4) and (5) were used to correct eq. (1) for this effect so that Darcy's law for the foam can be rearranged:

$$\frac{\Delta P}{L} = \frac{\mu A}{F(\epsilon)} v \tag{6}$$

where A is either A_c or A_f and $F(\epsilon)$ is a function of porosity and is equal to $\epsilon^3/(1-\epsilon)^2$ if the Carman–Kozeny equation is used [eq. (2)] or is equal to $\epsilon/(1-\epsilon)$ if the fiber drag equation [eq. (3)] is used. $F(\epsilon)/A$ is then identical with K.

Since the Reynolds number that defines the transition between laminar and turbulent flow in porous media is not well defined,[19] a semiempirical approach is used to describe the inertial contributions to the pressure gradient,[20]

$$\frac{\Delta P}{L} = Cv^2 \tag{7}$$

where C is a constant. C has been interpreted by Gent and Rusch in terms of average cell diameter and the diameter of the orifice between cells.[5] Gent and Rusch treated turbulent effects in flow through flexible foams as a series of expansions and contractions as the fluid passes through flow channels of irregular diameters.

Deviations from Darcy's law at very low velocities have also been observed for flow through foams.[6] This "flapper valve" effect arises because of the energy lost as the fluid must push aside broken or loose struts ("flapper valves") that obstruct the flow path. The theory derived for these losses yields

$$\frac{\Delta P}{L} = Bv^{0.4} \tag{8}$$

where B is a constant, although experiments yielded exponents ranging from 0.36 to 0.50.[21] B depends on pore geometry, strut thickness, cell size, fluid density, and the elastic modulus of the matrix. Although the theory was derived for flow of an ideal gas, it worked eqully well for both gases and liquids.

Combination of eqs. (6)–(8), modified according to eqs. (4) and (5), yields a generalized equation

$$\frac{\Delta P}{L} = \frac{\mu A}{F(\epsilon)} v + Bv^{0.4} + Cv^2 \tag{9}$$

which combines the viscous loss term with inertial losses and flapper valve losses to give the total pressure gradient at each value of velocity over the complete range of velocity. The validity and applicability of eq. (9) to flow-through hydrophilic polyurethane foams was tested in this study.

MATERIALS AND METHODS

Sample Preparation

Hydrophilic polyurethane foams were prepared in both rectangular and cylindrical molds with varying ratios of Hypol FHP3000 (W. R. Grace, Lexington,

MA), water and L520 surfactant (Union Carbide, Toronto). Surfactant and prepolymer were mixed initially with a mechanical four-blade impeller, followed by the addition of water and further mixing. The cream was poured into the molds and allowed to cure for 1 hr at room temperature.

The foams were sliced in a bandsaw to the required thickness and then frozen in liquid nitrogen; samples were punched out from the frozen slices with a cylindrical die on a drill press. In this way, the surface skin and other anomalies were avoided. The variation in dimensions was generally less than ±5% for each sample. Samples with obvious cracks or flaws were discarded.

For the permeability measurements, the lateral surfaces of the foams were sealed with two layers of Silastic E-RTV mold-making rubber (Dow-Corning, Toronto) and with a polyvinyl-acetate latex layer (National Adhesives X-Link Resyn, National Starch and Chemical, Toronto) between the two rubber layers.

A Silastic gasket was attached to the lower surface of the foam by either flaring the second lateral coating of Silastic or by gluing a separately made gasket. This gasket enabled sealing of the foam into the hydraulic permeability apparatus without leakage.

Sample Characterization

The foam porosity was determined by comparing the weight and volume of the dry foam with the matrix density determined in a pycnometer. The amount of water absorbed by the foam was also determined after repeatedly squeezing the foam in distilled water until no further release of air bubbles was observed and then maintaining it in water overnight. Swollen foams made without sur-

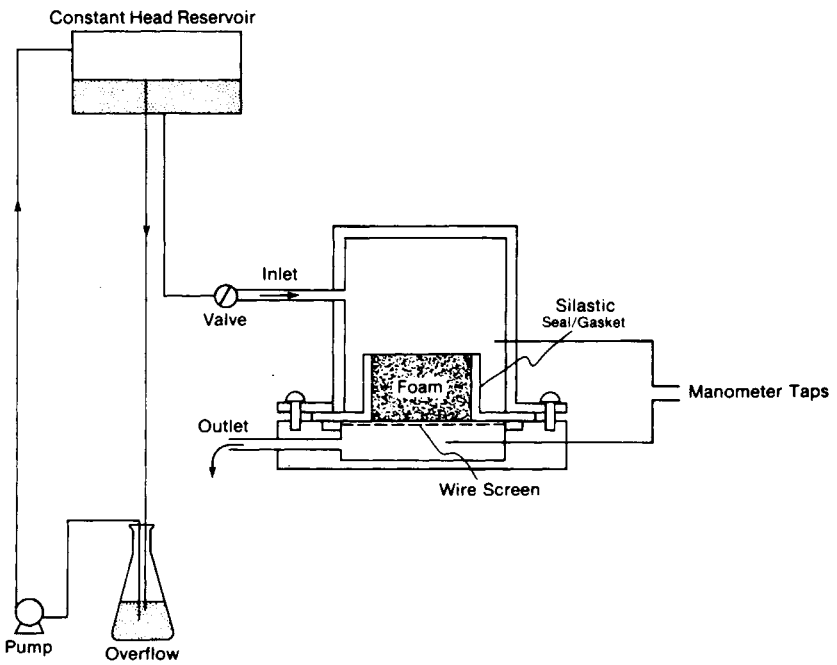

Fig. 1. Schematic diagram of permeability cell and apparatus.

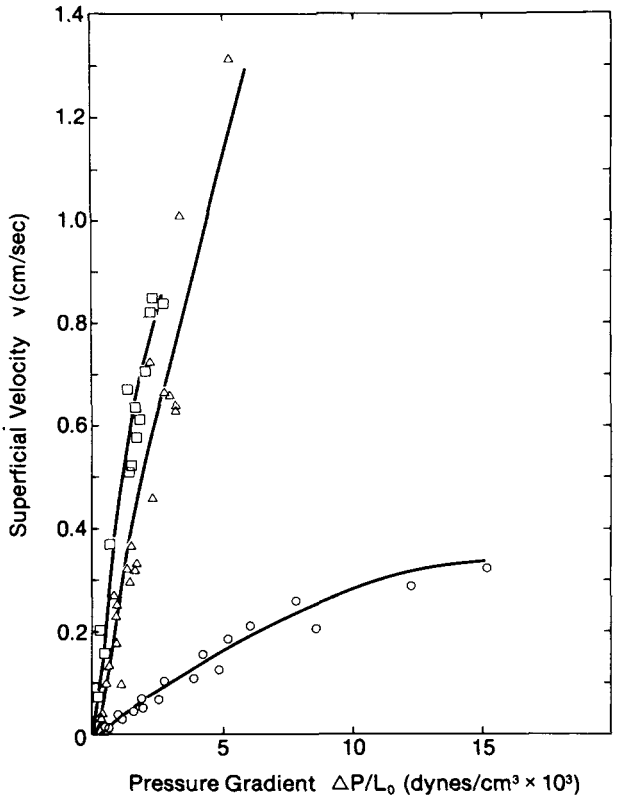

Fig. 2. Averaged effect of pressure gradient on velocity for foams of varying surfactant content. Experimental data: □, 100/70/0; △, 100/70/1; ○, 100/70/2. Foams were prepared in rectangular molds.

factant could not be weighed because of the rapid loss of water from their especially large pores.

The modulus of the swollen foam with lateral seal was estimated by direct observation of the compressive strain with a cathetometer as weight was applied to the top of the foam.

Permeability Determination

The foam with attached Silastic gasket was fitted between the flanges of the permeability cell (Fig. 1) under water. Particular attention was paid to the elimination of air bubbles in the foam and on keeping such bubbles from reentering the foam. The low-pressure output from the cell was collected in a graduated cylinder while either mercury/water or carbon tetrachloride/water manometers were used to measure the pressure drop across the foam. A constant head reservoir and valve were used to control the upstream pressure.

Measurements were begun at the highest possible flow rate to further purge the foam of any remaining air bubbles. It typically took 20–30 min for steady state to be reached and readings of flow rate and pressure drop were taken at steady state for the next 20–60 min. The flow rate would then be lowered and the measurement procedure repeated. Occasionally, the permeability cell was

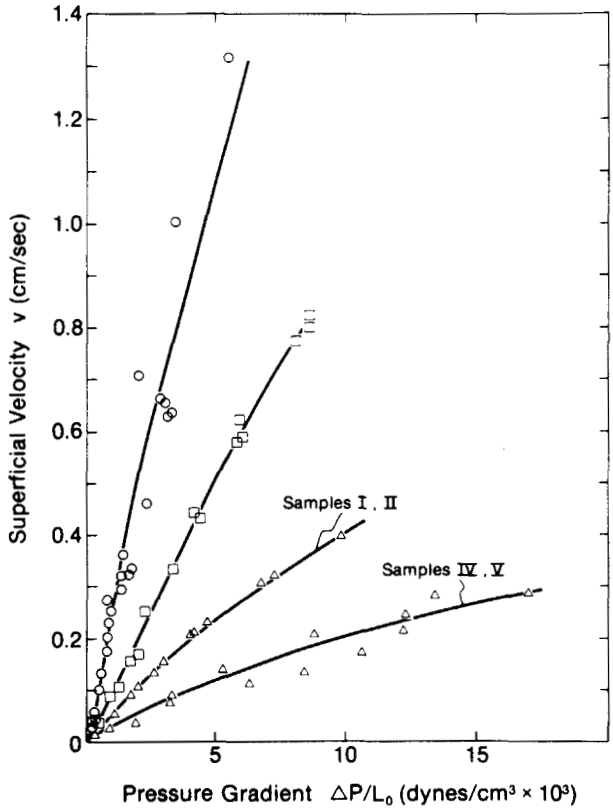

Fig. 3. Averaged effect of pressure gradient on velocity for foams of varying water content. Experimental data: △, 100/50/1; □, 100/125/1; ○, 100/70/1. Foams prepared in rectangular molds.

disassembled between runs, the foam reequilibrated with water by squeezing, and the apparatus reassembled again with the same foam: generally, no effect of this reequilibration was noted, indicating the absence of any air bubbles during testing.

RESULTS AND DISCUSSION

Average Permeability

The effects of surfactant content, prepolymer content, and foam mold on hydraulic permeability are shown in Figures 2, 3, and 4, respectively. It is clear from these curves that Darcy's law is not observed since the slope of these curves (i.e., the permeability) is not constant. It is believed that the permeability decreased at high gradients because of inertial effects and at very low gradients because of flapper-valve effects. Because these low gradient effects are minor (they are more obvious in Figs. 5 and 6), a linear relationship between velocity and pressure gradient was assumed to calculate an average initial Darcian permeability and the corresponding specific surface area according to the Carman–Kozeny interpretation of permeability (Table I).

It is clear from these results that an increase in permeability is correlated with cell size (that is, inversely with the specific surface area). For example, the in-

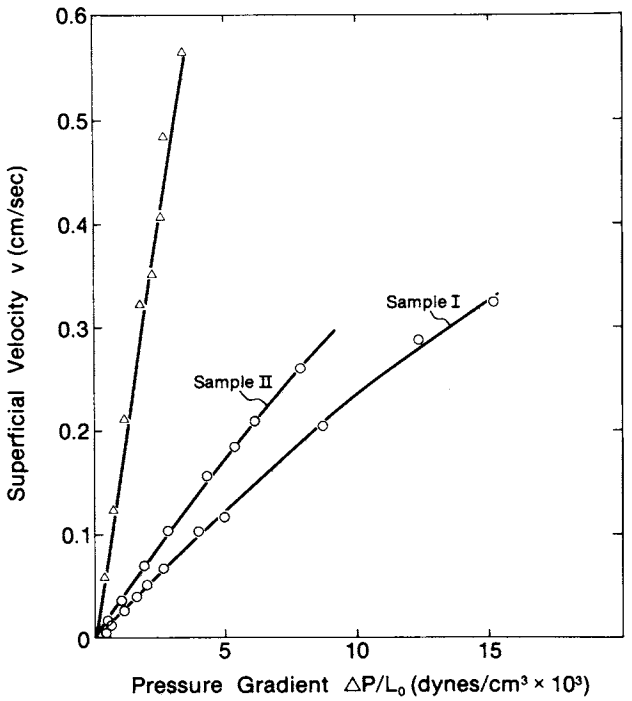

Fig. 4. Averaged effect of pressure gradient on velocity for foams prepared in different molds. Experimental data: O, rectangular mold; △, cylindrical mold. Formulation was 100/70/2.

corporation of surfactant in the foam formulation resulted in a reduction in average cell diameter and a corresponding decrease in permeability, even though the porosity was not much affected. Similarly, the recommended prepolymer content (100/70 water:prepolymer ratio) gave a foam with the largest cell size and largest permeability.

The effect of the foam growth mode may not be strictly a cell-size effect as suggested here but may be the result of a difference in cell orientation during flow measurement. Because of viscous effects during foam growth, the cells were generally nonspherical and oriented parallel to the growth direction. Foams prepared in a cylindrical mold had their cells oriented parallel to the flow direction during permeability measurement. Consequently, there were fewer obstructions to flow through the foam and the flow resistance was lower than in the foam prepared in a rectangular mold. For the latter foams, the cells were oriented perpendicular to the flow direction and many obstructions to the flow were encountered.

The scatter evident in the 100/50/1 and the 100/70/2 curves (Figs. 3 and 4) was primarly due to the variation in pore structure in each sample of foam made according to this formulation. This sample-to-sample variation is thought to be due to local mixing effects during the preparation of the foams giving rise to occasional defects (e.g., larger than normal pores) which dominate the permeability behavior by providing "short circuit" pathways through the foam. Whether these sample-to-sample variations are more significant for these formulations than for the others is unclear, however.

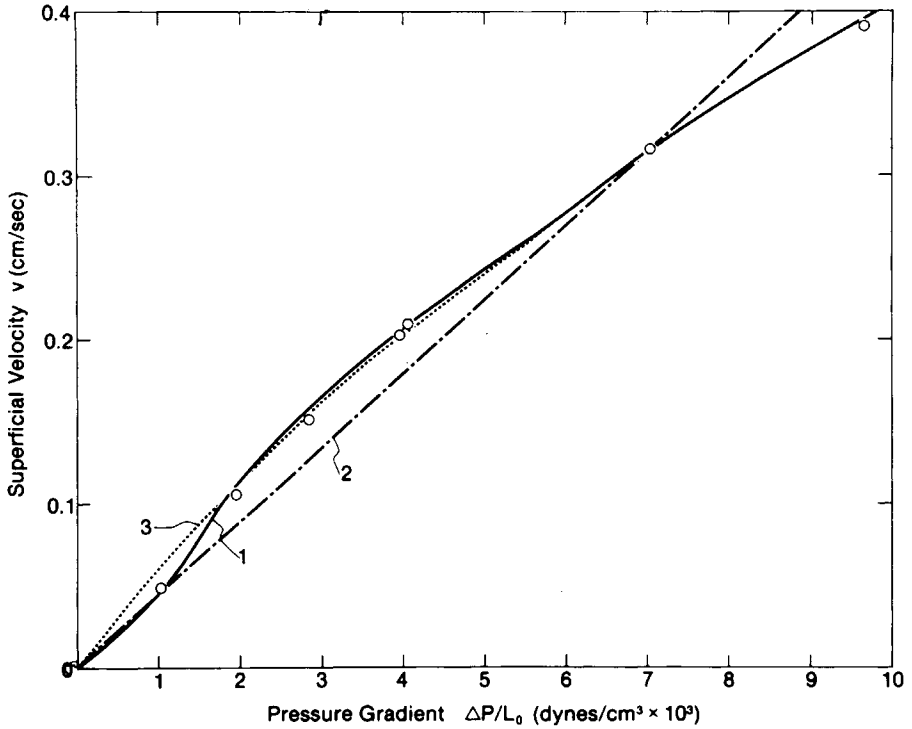

Fig. 5. Comparison of experimental and calculated data, for sample I of the 100/50/1 foam, according to eq. (9) and the indicated modifications of that equation. Calculated values are obtained from the equation which best fits the experimental data, O. Curve 1, eq. (9); curve 2, viscous term only ($B = C = 0$); curve 3, viscous and inertial terms only ($B = 0$).

Energy Losses

The three-term gradient/velocity equation [eq. (9)] was used to fit the experimental results for each foam sample. A direct-search procedure with search-region contraction was used to find the best values of A, B, and C that fit the experimental data by minimizing the sum of the squares of the deviations. An internal iteration was needed because the effect of the pressure gradient on porosity and foam length made the resulting equation implicit in pressure gradient. An optimum solution was also obtained for certain cases, with the flapper valve term and/or the inertial term set equal to zero. Typical results of this calculation are shown in Figure 5, where the model curves are compared with the experimental data.

The effect of foam compressibility was generally negligible for all of the samples. The porosity was typically reduced by approximately 0.001 over the experimental range of the pressure gradient. As a result the Darcian curve (i.e., best fit curve with $B = C = 0$) was virtually linear. The most notable effect was the curvature at higher velocities (higher gradients) evident in Figure 5, because of inertial effects ($C \neq 0$). At higher velocities, turbulence in the foam became significant, resulting in lower permeabilities than in the Darcian (viscous) range. No specific velocity (or Reynold's number) which defined the transition from laminar to turbulent flow was identified from these results.

Since there are only one or two experimental points in the low-gradient region, where the flapper valve term is important, inspection of Figure 5 might suggest

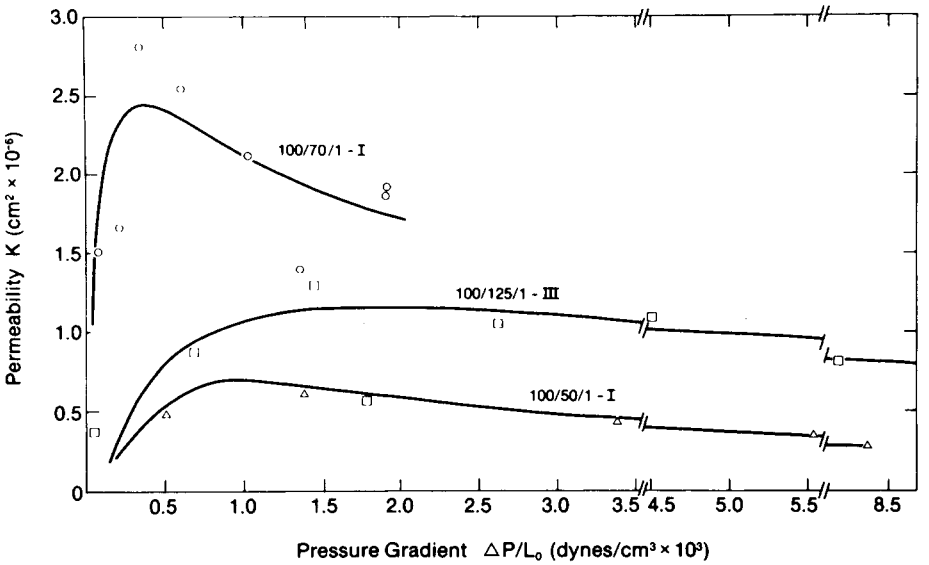

Fig. 6. Comparison of experimental and calculated permeabilities. Experimental values from the slope of the chord joining each pair of data; calculated values from the derivative of eq. (9) using the best fit parameters. Experimental results: ○, 100/70/1-I, □, 100/125/1-III, △, 100/50/1-I.

that this term could be neglected without having much effect on the overall degree of fitness of the model. A plot of experimental and model permeabilites, however, shows a definite maximum at low gradients (Fig. 6). The experimental gradients were calculated from the slope of the chord joining each successive pair of experimental values giving rise to a great deal of scatter; the model curve was plotted using the derivative of eq. (9). In the absence of flapper valve effects, the permeability should rise monotonically as the gradient is lowered and then level off at a constant value indicative of pure viscous (Darcian) effects. The indicated decrease at very low gradients was evidence of the presence of another energy consumption process which is important only at these low gradients and was presumed to be a flapper valve effect.

The range of best fit values for B and C from the three-term equation are listed in Table I, for each formulation. In general, the inertial term constant C correlated inversely with the average permeability, and thus, inversely with the pore diameter of the foam: the higher the pore size, the higher the average permeability and the lower the values of C. Since contraction losses were primarily accounted for in this term and these losses depend on the number and relative size of the openings between pores, these results suggested that the smaller the pore diameter, the greater the contraction losses associated with the flow of water from one foam cell to the next.

The flapper valve constant B showed the greatest variability particularly for the 100/70/1 foams. Since this term arises from the energy losses in pushing aside loose struts, it is plausible to presume that this term would be more sensitive to sample-to-sample variations. However, the source of this variation must be different than that affecting the Darcian term since the 100/50/1 foams had the greatest variation in A, but a relatively small variation in B.

TABLE I
Permeability Properties of Hypol Foams

Formulation	Average porosity[a]	Average initial permeability,[b] ($cm^2 \times 10^{-6}$)	Specific surface area of foam[c] ($cm^2/cm^3 \times 10^3$)	Velocity/pressure gradient parameters[d] range ($\times 10^2$) B	C
		Varying surfactant			
100/70/0[e]	0.915	3.8	3.8	0.88–0.98	6.8–2.5
100/70/1	0.936	2.3	6.6	0.59–5.6	7.9–19
100/70/2	0.929	0.32	15.8	13.4–47	249–496
		Varying water			
100/50/1	0.943	0.34	19.5	5.4–23.4	268–744
100/125/1	0.932	1.0	9.3	7.5–17.6	37.6–51.7
100/70/1	0.936	2.3	6.6	0.59–5.6	7.9–19
		Varying growth orientation			
100/70/2	0.929	0.32	15.8	13.4–14.7	249–496
100/70/2C	0.934	1.8	7.3	—	—

[a] Porosity based on dry weight of bulk foam; average for all samples.

[b] Average initial permeability calculated from slope of straight line drawn through low-gradient region (<5000 dyn/cm^3) of permeability curves; effects of compressibility and sample-to-sample variations were ignored.

[c] Specific surface area, based on Carman–Kozeny form of Darcy's law [eq. (2)] assuming tortuosity $\tau = 1$.

[d] Parameters are defined by eq. (9) and calculated from the best fit of experimental data (Units: v, cm/sec; $\Delta P/L$, dyn/cm^3).

[e] Formulation given as wt water/wt prepolymer/wt surfactant; C refers to preparation in cylindrical molds.

Interpretations of Darcian Permeability

The Darcian permeability at zero gradient was calculated from the best fit value of A and $F(\epsilon)$ according to eq. (2).

As was true for the average permeabilities (Table I), the Darcian permeabilities at zero gradient of each sample also exhibited an inverse dependence on the specific surface area calculated according to the Carman–Kozeny equation (Fig. 7), without any correlation with porosity. Hence, the hydraulic permeability of individual foam samples was primarily dependent on cell size (specific surface area) and not porosity, with smaller pore size foams having lower permeabilities.

Alternatively, the fiber drag model [eq. (3)] was used to interpret the Darcian permeabilities at zero gradient. As permeability increased, the calculated value of the fiber diameter, δ, increased (Fig. 7), indicating that viscous drag on the matrix struts, modeled here as a bundle of fibers, decreased. To the extent that δ can be considered as an average strut diameter, the hydraulic permeability is thus related to the strut diameter, as an alternative to cell size, with foams with larger strut diameters having higher permeabilities.

The Peterlin model[22] for the hydraulic permeability of highly swollen membranes was also used to interpret the results. Surprisingly, despite the great structural differences between these foams and the highly swollen membranes of Peterlin, the permeabilities at zero gradient plotted against the ratio $(H/1 - H)$ where H is the volume fraction of water absorbed by the foam yielded a straight line (albeit, the correlation coefficient = 0.72) with a slope of 5.75×10^{-7}

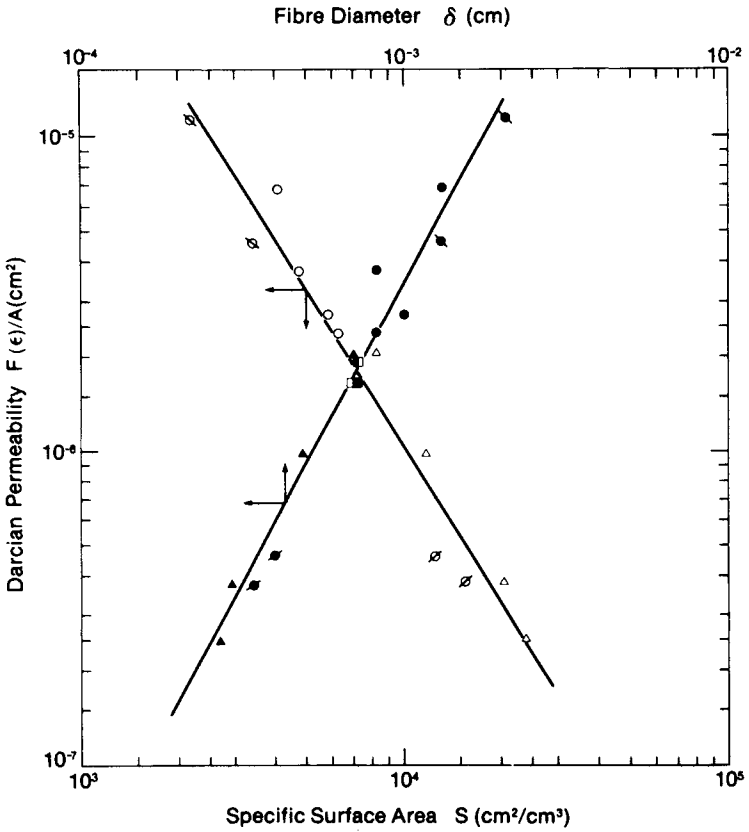

Fig. 7. Correlation of Darcian permeability, $F(\epsilon)/A$, with specific surface area, S, calculated according to the Carman–Kozeny equation (2) and with fiber diam δ, calculated according to eq. (3). ○, ●, 100/70/1; △, ▲, 100/50/1; □, ■, 100/125/1; ⌀, ⌀ 100/70/0; ⌀, ⌀ 100/70/2.

and abscissa intercept of 1.25. Although the slope cannot be interpreted in terms of a molecular frictional coefficient, the presence of a linear correlation does suggest that a single frictional coefficient can be assigned to all samples of the foam regardless of formulation or other intra-sample variations. This frictional coefficient represents the individual contribution of a characteristic subunit of these foams to the total viscous resistance. Presumably, this characteristic subunit has some relationship to the individual foam cell.

CONCLUSIONS

The hydraulic permeability of open-cell hydrophilic polyurethane foams were very sensitive to foam formulation and to the mode of preparation. Furthermore, sample-to-sample variations were readily determined. In addition to viscous losses, other energy losses attributed to inertial effects and to the pushing aside of loose foam struts, were apparent at high and very low gradients, respectively. These nonviscous losses were somewhat more sensitive to sample-to-sample variations.

The viscous loss term (Darcian permeability) was readily interpreted in terms of cell size or specific surface area using the Carman–Kozeny equation, suggesting

that the permeability of these foams was strongly dependent on cell size rather than porosity. Alternative explanations, however, were also reasonable; for example, the fiber-drag model of flow-through porous media was applied to these results, suggesting a correlation between foam permeability and strut diameter. Although the Carman–Kozeny model is more convenient and more widely used, no clear preference for one model or the other can be justified on the basis of these results.

The authors wish to thank the Natural Sciences and Engineering Research Council for the support of this work and for a fellowship to H. M. L.

References

1. B. Richter and R. Voigt, *Pharmazie*, **29**(1), 3 (1974).
2. G. Moll, Koll. *Z. & Z. Polym.*, **203**(1), 20 (1965).
3. J. G. Helmcke, *Zentr. Bakteriol., Abt. 1.*, **159**, 308 (1953).
4. V. Hampl and K. Spurny, *Collect. Czech. Chem. Commum.*, **31**, 1152 (1966).
5. A. N. Gent and K. C. Rusch, *J. Cell. Plast.*, **2**(1), 46 (1966).
6. J. P. Bosscher and R. E. Fisher, *J. Cell. Plast.*, **6**(6), 275 (1970).
7. E. F. Cuddihy and J. Moacanin, *J. Cell. Plast.*, **3**(2), 73 (1967).
8. B. S. Mehta and E. A. Colombo, *Soc. Plast. Eng. Tech. Papers*, **24**, 689 (1978).
9. R. H. Harding, *J. Cell. Plast.*, **1**(1), 224 (1965).
10. (a) R. G. Griskey, *AIChE Symp. Ser.*, **73**(170), 158 (1977).
11. (a) E. Bettanini, A. Cavallini, and P. DiFilippo, *Int. Congr. Refrigeration Proc.*, **12**(2), 159 (1967); (b) E. Bettanini, *Int. Congr. Refrigeration Proc.*, **12**(2), 169 (1967).
12. M. V. Sefton and J. L. Mann, *J. Appl. Polym. Sci.*, **25**, 829 (1980).
13. M. V. Sefton, H. M. Lusher, S. R. Firth, and M. U. Waher, *Ann. Biomed. Eng.*, **7**, 329 (1979).
14. M. V. Sefton, "Makro Mainz", in *Prepr. IUPAC Conf.*, **3**, 1543 (1979).
15. J. L. Guthrie, U.S. Pat. 3,861,993, 1975.
16. *Hypol Laboratory Procedures and Foam Formulations* W. R. Grace, Cambridge, MA, 1976.
17. A. E. Scheidegger, *The Physics of Flow Through Porous Media*, 3rd ed., University of Toronto Press, Toronto, 1974, p. 141.
18. A. S. Iberall, *J. Res. Natl. Bur. Stand.*, **45**, 398 (1950).
19. A. E. Scheidegger, *The Physics of Flow Through Porous Media*, 3rd ed., University of Toronto Press, Toronto, 1974, p. 154.
20. P. Forchheimer, *Z. Ver. Deuts. Ing.*, **45**, 1782 (1901).
21. J. P. Bosscher, personal communication, 1977.
22. A. Peterlin, H. Yasuda and H. G. Olf, *J. Appl. Polym. Sci.*, **16**, 865 (1972).

Received February 15, 1980
Accepted May 16, 1980